## Spectral analysis of blood stains at the crime scene

Edelman, G.J.

**Publication date**
2014

# 3 - REFLECTANCE SPECTROSCOPY AND HYPERSPECTRAL IMAGING FOR THE IDENTIFICATION OF BLOOD STAINS

Partly published in:
Journal of Forensic Science 2011;56(6):1471-5
Proc. SPIE 8743 2013;doi:10.1117/12.2021509

We demonstrated the feasibility of reflectance spectroscopy and hyperspectral imaging to detect and identify blood stains remotely at the crime scene. Blood stains outside the human body comprise the main chromophores oxyhaemoglobin, methaemoglobin and hemichrome. Consequently, the reflectance spectra of blood stains are influenced by the composite of the optical properties of these individual chromophores. Using the coefficient of determination between a non-linear least squares multi-component fit and the measured spectra, blood stains were successfully distinguished from other substances visually resembling blood (e.g. ketchup, red wine and lip stick) with a high sensitivity and specificity. The practical applicability of this technique was demonstrated at a mock crime scene, where blood stains were successfully identified automatically. Finally, the described technique was applied in a case example, in which a stain on a paint can was tested for the presence of blood.

## 3.1. INTRODUCTION

Identification of blood stains at a crime scene is of critical importance in criminal investigations. Extraction of DNA from the stains may lead to the identification of victims or suspects, and the blood stain pattern can reveal useful information about the activities needed to produce these patterns. To avoid contamination and destruction of traces, there is a need for techniques that allow for remote, non-contact identification of blood. Ideally, traces are judged and interpreted in the original context, so techniques are preferably applied at the crime scene[74].

Various screening tests, routinely used in forensic practice, use chemical or optical methods for the identification of blood and to discriminate it from other body fluids or red substances. Most chemical tests, including tetrabase[75] and Kastle-Meyer, employ peroxidase activity of haemoglobin molecules. The peroxidase either causes a colour change or induces chemiluminescence. A commonly used example of the latter is the luminol test. By spraying luminol onto the suspected area, the reactant will glow in the presence of blood[76]. This test is especially appropriate for recovering stains after cleaning attempts. All tests described above are presumptive in nature, not confirmative, since several other substances are reported to catalyze this peroxidase reaction[77]. More reliable, confirmatory tests are based on haemoglobin derivative crystals[78, 79] or RNA markers in blood[80]. However, these tests require advanced sample preparation and microscopic observation, and are therefore not applicable for interpreting traces in their original context, at the crime scene.

Recently, optical techniques have been suggested for blood stain identification[70, 81]. Haemoglobin has specific absorption bands at 420 (known as the Soret band), 540 and 576 nm (attributed to the α and β chains in a haemoglobin molecule)[82]; it fluoresces at 465 nm, when exited at 321 nm[83]; and haem provides Raman shifts[84] at 1.222 and 1.542 $cm^{-1}$. Because of these specific optical features of haemoglobin, spectroscopic techniques, e.g. visible reflectance, fluorescence or Raman spectroscopy, have the potential to allow on field identification of blood. However, despite the promising results, these

techniques have not been reported to be implemented in forensic practice yet. Accordingly, all these techniques have their own drawback. Measuring Raman signals is highly complicated by interference with the fluorescence signal of the traces and its background. A fluorescence signal is difficult to measure, because of the high absorption properties of haemoglobin in the ultraviolet and visible wavelength range. The value of the absorption properties for blood stain identification has been demonstrated by Kotowski *et al* in a microspectrophotometry setup[85]; De Weal *et al* recently confirmed their findings[81]. Their microscopic setup however, required sample preparation and a laboratory environment for accurate measurements.

In this study, we investigated whether blood stains can be detected and discriminated from other body fluids and substances visually mimicking blood, based on their visible reflectance spectra. In a laboratory setup, the reflectance spectra of a set of blood samples and a set of mainly red/brown coloured substances were measured using both conventional probe based optical reflectance spectroscopy and hyperspectral imaging. Hyperspectral imaging combines spectroscopy with imaging, thereby obtaining both spatial and spectral information from all objects in the field of view. When analyzing blood stains, the added spatial information is interesting, as the blood stain patterns can reveal useful information for the reconstruction of a crime and all stains can be interpreted in their original context. Hyperspectral imaging also improves the speed of the process compared to spectroscopy, as many samples can be recorded and analysed at once.

The spectral analysis applied in this chapter was based on the expected presence of haemoglobin derivatives in blood. Blood stains outside the human body comprise mainly the chromophores oxyhaemoglobin, methaemoglobin and hemichrome[1]. We used a physical light transport model and a fitting algorithm to find a combination of haemoglobin derivatives leading to a reflectance spectrum most similar to the measured spectrum. Assuming that all blood stains contain a mixture of these haemoglobin derivatives, the fitted spectra were expected to resemble all measured spectra of blood stains. Worse fits were expected for non-blood samples. Therefore, the goodness-of-fit was evaluated as a measure to distinguish blood from other samples. The sensitivity

and specificity of this method were analyzed in a laboratory setup, both for the probe based spectroscopy and the hyperspectral imaging setup. Based on experiences using the spectroscopy setup, the data analysis was slightly improved for the hyperspectral imaging setup. At a mock crime scene, we investigated the practical applicability of this technique using hyperspectral imaging. Finally, the spectroscopy setup was applied in a forensic case, to determine whether an unknown stain on a paint can was blood or not.

## 3.2. PROBE BASED SPECTROSCOPY

### 3.2.a MATERIALS AND METHOD

#### Samples

To test the sensitivity and specificity of the blood stain identification task using spectroscopy, two sample sets were prepared: a set of blood samples and a set of blood mimicking samples and different body fluids. The blood samples, forty in total, were obtained from eight healthy male donors. These samples were prepared by deposition of a small drop of blood onto a piece of white cotton, creating a stain with a diameter of 21 ± 4 mm. We performed 1200 measurements on the forty blood samples, covering a period of a few seconds after deposition until a year after deposition; this resulted in thirty measurements per sample, to monitor possible influences of ageing.

The second set contained 35 non-blood samples (specified below in Figure 3.4). Among these samples were 31 samples mimicking blood visually, including ketchup, red wine and fake blood; and four body fluids commonly found at crime scenes: saliva, semen, urine and perspiration. All samples were created, similar to the blood stains, onto a piece of white cotton.

#### Measurement setup

Reflectance measurements were performed with a combination of a spectrograph (USB 4000; Ocean Optics; Duiven, the Netherlands), a tungsten-halogen light source (H-2000; Ocean Optics; Duiven, the Netherlands) and a

non-contact probe (QR400-7-UV/BX; Ocean Optics; Duiven, the Netherlands). This probe contains six 400 μm core diameter delivery fibres, circularly placed around a similar central collecting fibre. Figure 3.1 shows the schematic of the setup. The probe is positioned 1 cm above the specimen. During measurements, light emitted by the delivery fibres is scattered and partly absorbed in the sample, and the remitted light is collected with the central fibre.

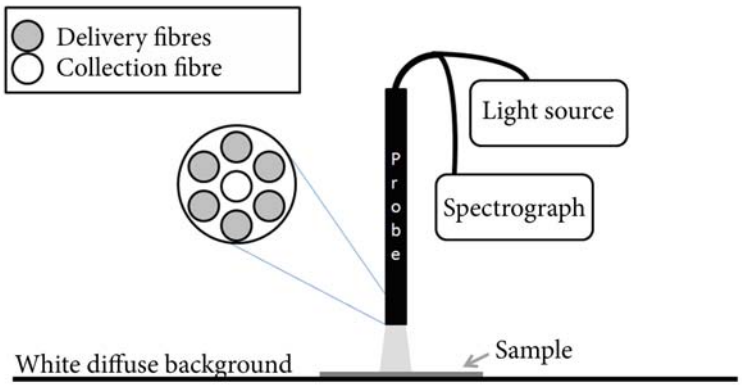


Figure 3.1. Schematic of the measurement setup. The reflection probe tip shows six delivery fibres, placed around a central collection fibre. The delivery fibres are connected to the light source and the collection fibre is connected to the spectrograph.[65]

## Pre-processing

Spectral analysis was limited to the wavelength range of 500 – 700 nm, because of the low detector sensitivity and low power of our light source beyond this range. First, the dark response ($I_{dark}(\lambda)$) of the detector was subtracted from each spectrum. Next, to account for the intensity spectrum of the light source, we divided by the background response of white cotton at all wavelengths ($I_{white}(\lambda)$):

$$R(\lambda) = \frac{I\ (\lambda) - I_{dark}(\lambda)}{I_{white}(\lambda) - I_{dark}(\lambda)}, \tag{3.1}$$

where $R$ is the reflectance and $I$ is the intensity.

**Blood stain identification**

The reflectance spectra were analyzed with a multi-component linear least squares fit. The absorption spectra of the three components present in blood, i.e. oxyhaemoglobin, methaemoglobin and hemichrome (Figure 3.2) were used as input.

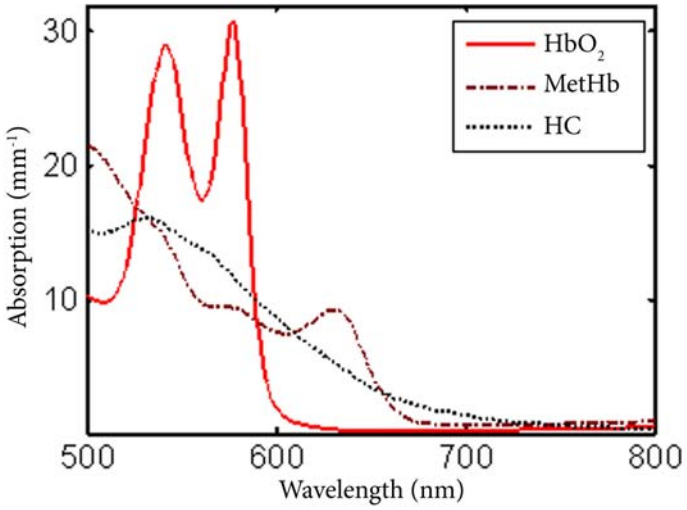


Figure 3.2. Absorption spectra of oxyhaemoglobin ($HbO_2$), methaemoglobin (MetHb) and hemichrome (HC)

A one-dimensional solution of the radiative transport theory was employed to translate these spectra into a reflectance spectrum:

$$R = 1 - \frac{K}{S}\left(\sqrt{1+\frac{2S}{K}} - 1\right), \tag{3.2}$$

where $R$ (-) is the reflectance, $S$ ($mm^{-1}$) is derived from the scattering coefficient, and $K$ ($mm^{-1}$) from the absorption coefficient[86, 87]. This model

assumes a homogeneous blood layer of infinite thickness interacting with incoming diffuse light. The fitting algorithm varies the amplitudes of the three absorption spectra, in order to find the combination with a minimum of difference between the theory and the diffuse reflectance spectrum[1].

Assuming that all blood stains contain a mixture of haemoglobin derivatives, the non-linear least squares fit was expected to resemble all measured spectra of blood stains. Worse fits were expected for non-blood samples. The goodness of fit was determined using the coefficient of determination $R^2$ and the sensitivity and specificity of the identification tasks were studied.

To test on differences in $R^2$ values within the total blood stain population three individual, one way ANOVA tests were taken on samples (n=40), donors (n=8) and ageing. For ageing testing, we grouped the blood stains in four categories: age <1 day; 1 day < age < 1 week, 1 week < age < 1 month and age > 1 month. Significance is found if $p < 0.05$.

### 3.2.b RESULTS

The left hand side of Figure 3.3 shows a typical diffuse reflectance spectrum of a blood sample of one day old, measured with the spectroscopy setup. The spectrum shows two distinct dips, at 540 nm and 576 nm, corresponding to the oxyhaemoglobin absorption maxima[82]. The calculated coefficient of determination between the blood reflectance spectrum and the blood component fit is very high: $R^2=0.996$. The reflectance spectra of all blood samples were obtained and all corresponding coefficients of determination were calculated. For the total of 1200 measurements we found an average $R^2$ of $0.986\pm0.012$.

Three one-way ANOVA tests were performed to test on differences in sample, donor and ageing. The outcome of the test shows that at a 0.05 level, no significant difference is found among sample variation (F-value = 0.8014, prob >F = 0.8040) and donor variation (F-value = 0.8215, prob >F = 0.569). However, for ageing, a significant difference is found (F-value = 64.4, prob >F = 0). For both ages smaller than one day and ages between a day and a week $R^2$

=0.99±0.01; for ages between a week and a month and older than one month $R^2$ =0.98±0.01. This difference in $R^2$-value between stains measured within a week and after a week of deposition is found significant at a 0.05 level.

The right hand side of Figure 3.3 shows a reflectance spectrum of a blood mimicking sample: ketchup. The agreement between the sample's reflectance spectrum and the blood-fit is poor, especially for $\lambda$<600 nm. The poor agreement results in a low coefficient of determination: for the total population of 35 non-blood samples the average $R^2$=0.67±0.21 was found.

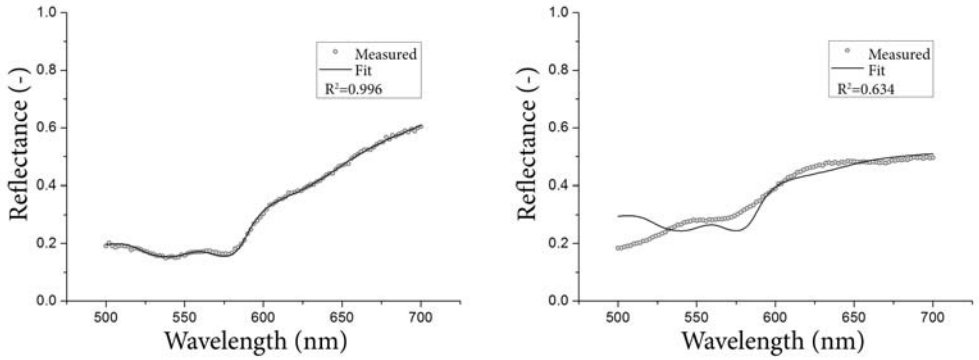


Figure 3.3. Diffuse reflectance signal (grey dots) with corresponding blood-fit (black line). Two typical measurements are shown: a) a blood sample of one day old and $R^2$=0.996 b) a non-blood sample: ketchup, $R^2$=0.634.[65]

Figure 3.4 shows the coefficients of determination of four typical blood stains and all non-blood samples. The blood samples, coloured in black in Figure 3.4, have the following coefficients of determination: immediately after deposition, $R^2$=0.997; after one day: $R^2$=0.996; after one month: $R^2$=0.982 and after one year: $R^2$=0.984. The non-blood samples are coloured in grey. The non-blood samples with highest $R^2$ are coloured lip gloss: $R^2$=0.961 and red wine: $R^2$=0.954. Non-red body fluids, shown on the right side of figure 3, score low correlations, saliva: $R^2$= 0.199, semen: $R^2$=0.476 perspiration: $R^2$=0.669 and urine: $R^2$= 0.381. The patterned column on the far right resembles the measured $R^2$ of the case study, which will be discussed in detail below.

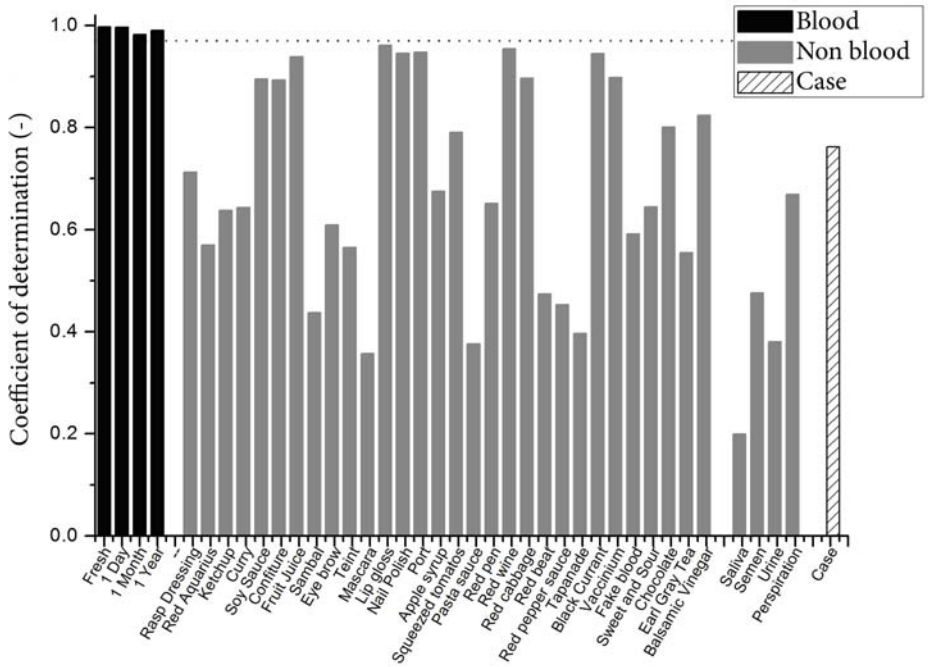


Figure 3.4. Column plot of coefficients of determination of four typical blood samples (black), all non-blood samples (grey) and case study (patterned).[65]

Figure 3.5 plots the distribution of the obtained $R^2$-values for all samples. The boxes show the distribution of 25%, 50% and 75% of the samples, the whiskers show 1% and 99% of samples. The coefficient of determination in Figure 3.5 is plotted on a logarithmic scale to enable visualization in both blood and non-blood samples.

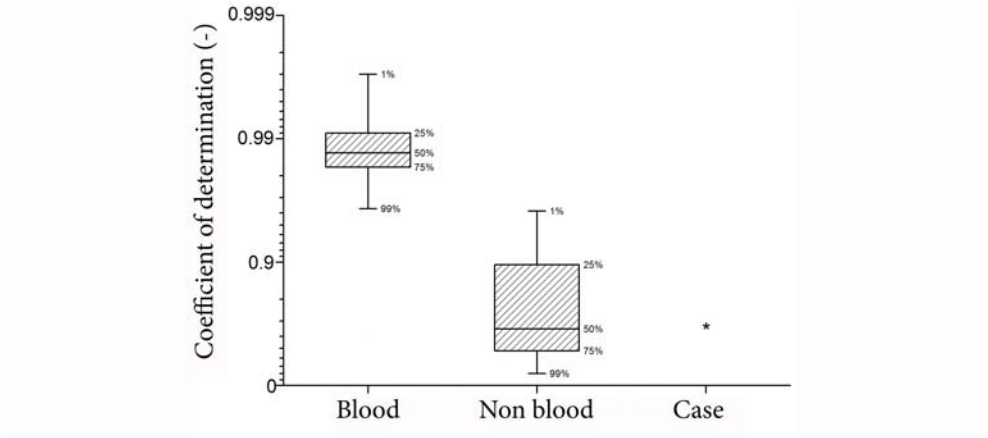


Figure 3.5. Box plot of the distribution of observed coefficients of determination of all blood measurements (n=1200) and all non-blood samples (n=35). On the right the outcome of the case example described below.[65]

A possible threshold for the separation of blood and non-blood samples would be at $R^2$=0.97. At this level, the specificity is 100% and the sensitivity 98.1%, i.e. no non-blood samples were reported with $R^2$>0.97 and only 1.9% of the blood samples were found to have $R^2$<0.97.

## 3.2.c CASE EXAMPLE

### Materials and method

The spectroscopy method presented in this chapter was applied for investigational purposes in a case where someone was suspected of multiple burglary cases. The paint can found at one of the crime scenes contained latent traces of a fingerprint, possibly printed in blood. Confirmation or exoneration of the nature of the stain was crucial for the processing of this particular crime. We measured the reflectance spectrum of the questioned stain and analysed it as described above to indicate whether it was blood. A tetrabase test was used for verification of the result.

**Result**

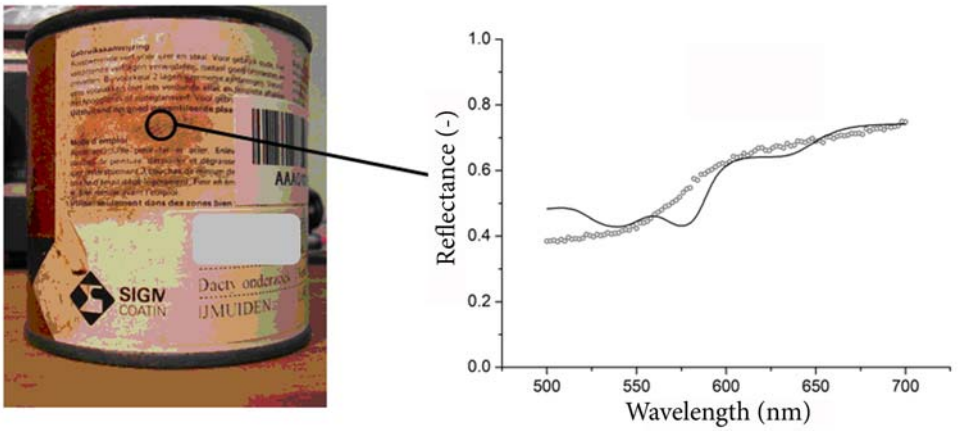


Figure 3.6. Left: Photograph of paint can of interest for blood test. The black line with open circle shows the spot where the reflectance spectrum is recorded. Right: Diffuse reflectance signal with corresponding linear least squares fit.65

Figure 3.6 shows a photograph of a paint can found at the crime scene. We obtained a diffuse reflectance spectrum of a red stain on this can and found an $R^2$-value of 0.672, which is much lower than the values found for blood (see Figure 3.5), indicating that the stain does not contain blood. To verify the optical presumptive test for this case example, an additional tetrabase test[75] was performed on the same spot. Tetrabase tests are routinely used in forensic practice in the Netherlands. According to the instructions, filter paper was used to sample a small amount of substance from the paint can. Thereafter the filter paper was treated with the tetrabase chemicals. The filter paper did not change colour after deposition of the tetrabase, indicating no presence of blood on the paint can. The tetrabase test was performed twice, once with dry filter paper, and once with wet filter paper. The results of the tetrabase test were in agreement with the outcome of the spectroscopic identification.

# 3.3. HYPERSPECTRAL IMAGING

## 3.3.a MATERIALS AND METHOD

### Samples

The samples used to test the hyperspectral imaging setup were similar to the set described above. Again, blood stains on white cotton were analysed repeatedly (every day for 4 weeks, thereafter weekly until the age of 2 months). The 30 different non blood samples are specified in Figure 3.7. Instead of the bodily fluids analysed using spectroscopy, bleach was added to the set, as bleach is likely to be false positive when using the commonly used identification technique luminol.


Figure 3.7. Photographs of non-blood samples containing: 1) tea, 2) coffee, 3) red wine, 4) red grape juice, 5) black currant soda ('cassis'), 6) coke, 7) cherry coke, 8) red berry juice, 9) tomato juice, 10) ketchup, 11) curry, 12) Tabasco, 13) ketjap manis, 14) Worstershire sauce, 15) soy sauce, 16) balsamic, 17) Maggi aroma, 18) red wine, 19) cherry marmalade, 20) forest fruit marmalade, 21) apple syrup, 22) chocolate sauce, 23) red cabbage, 24) red beet, 25) bleach, 26) lipstick, 27) lipstick, 28) lipstick, 29) red food colourant, 30) red food colourant.

### Measurement setup

The hyperspectral imaging system used was a push broom line-scanning system (Spectral Imaging Ltd., Oulu, Finland), consisting of a rotary stage, a hyperspectral camera operating in the visible- near infrared wavelength range (400-1000 nm) and a broadband halogen light source.

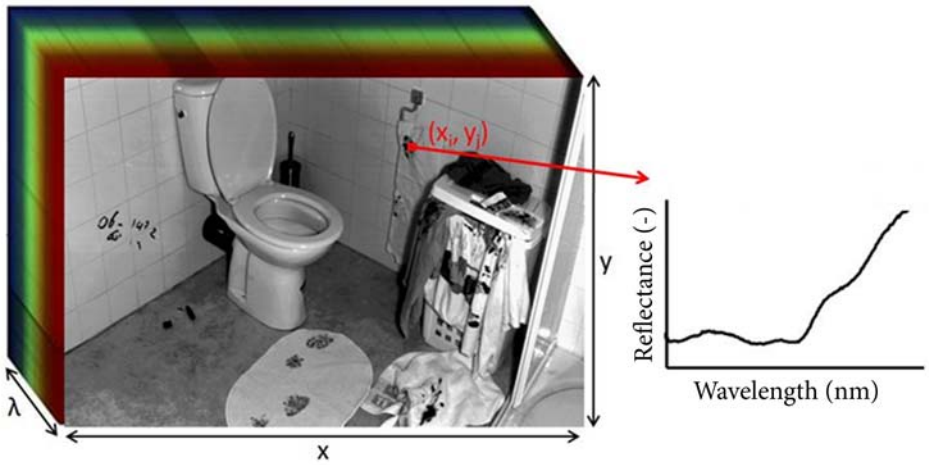


Figure 3.8. Hypercube of a mock crime scene, with two spatial (x, y) and one wavelength (λ) dimension (left). From the hypercube a reflectance spectrum was obtained from each pixel ($x_i$, $y_j$) (right).

Using this system, we recorded so-called hypercubes (explained in **Chapter 2**), containing two spatial dimensions (x, y) and a spectral dimension (λ) (see Figure 3.8). From these hypercubes, a region of interest of 10 x 10 pixels was cropped for each sample, corresponding to a sample size of approximately 1 $cm^2$. Reflectance spectra were obtained for all these regions as described below.

**Pre-processing**

In the hyperspectral imaging setup, the wavelength range was expanded to 500 – 800 nm. The reflectance spectra for all samples were calculated as above, with corrections for the dark response and light source (formula 3.1). Now, an extra correction algorithm, the Standard Normal Variate algorithm[14] was applied to normalize spectral variations caused by differences in sample-detector distance and variations in local light intensities:

$$R_{corr}(\lambda) = \frac{R(\lambda) - \mu}{\sigma}, \tag{3.3}$$

in which $R_{corr}$ is the corrected reflectance, $\mu$ the average reflectance and $\sigma$ its standard deviation.

**Blood stain identification**

The reflectance spectra of all samples were analyzed using the fitting algorithm described above (formula 3.2). To examine the goodness of fit between the measured reflectance spectra and the fitted light transport model, the coefficient of determination $R^2$ was calculated for each pixel of the different samples. A Receiver Operating Characteristic (ROC) curve was plotted, showing the sensitivity and specificity of the identification tasks at different thresholds of $R^2$.

## 3.3.b RESULTS

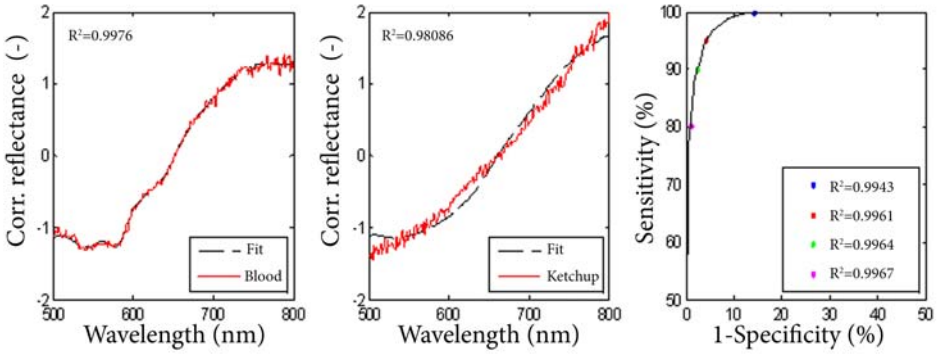


Fig. 3.9. a) Corrected reflectance spectra (red) of a single pixel depicting blood and the corresponding least squares fit (black). The $R^2$ value for this pixel is 0.9976. b) Corrected reflectance spectra (red) of a single pixel depicting ketchup and the corresponding least squares fit (black). The $R^2$ value for this pixel is 0.98086. c) ROC curve showing the sensitivity and specificity of the identification task at different thresholds. Coloured dots represent the sensitivity and specificity at several thresholds given in the legend (e.g. at $R^2$= 0.9943 the sensitivity is 100% and the specificity is 85%).

Fig. 3.9 shows the corrected reflectance spectra of two pixels depicting blood (Fig. 3.9a) and ketchup (Fig. 3.9b), and the corresponding non-linear least squares fits of the haemoglobin derivatives present in blood stains. Please note that for both cases the coefficients of determination $R^2$ between the fits and the measured reflectance spectra approach one, but this coefficient was lower for most non-blood stains than for blood stains.

The ROC-curve (Fig. 3.9c) shows the sensitivity and specificity of the identification task at different thresholds. At a threshold of $R^2$= 0.9943 we reached a sensitivity of 100% and a specificity of 85%. False positive pixels at this threshold contained ketjap manis, Worcestershire sauce, soy sauce, balsamic, red cabbage and bleach. The area under the curve (AUC) was 0.99.

### 3.3.c MOCK CASE EXAMPLE

#### Materials and method

Finally, we recorded a hyperspectral image of a mock crime scene (see Figure 3.10), in which red wine, lipstick and several blood stains of different ages were present. The pre-processing steps described above were applied to the data and all individual pixels were analysed using the non-linear least squares fitting algorithm. For each pixel the goodness of fit was measured using the coefficient of determination $R^2$. All pixels with an $R^2$ value above a predetermined threshold were coloured red in a mask, which was overlayed onto a greyscale background depicting the scene (one waveband of the hyperspectral image). False positive and false negative pixels of the mock crime scene were evaluated.

Figure 3.10. Greyscale image (one wavelength band of the hypercube), overlayed with red pixels showing identified blood stains at a threshold $R^2$ of 0.98.

At the mock crime scene a hypercube was recorded with 800 pixels in vertical direction, 1575 in horizontal direction and 424 spectral bands (2x2 binning), in less than two minutes. All individual pixels in the hypercube were analyzed as described above. At a threshold of 0.98, most blood stains were identified, as depicted in Figure 3.10. Several pixels which were later confirmed to contain blood on the blue T-shirt and on the cloth on the floor were not identified using hyperspectral imaging. False positive pixels contained 4 pixels of the lipstick on the wall and 6 pixels in the specular reflecting part on the waste pipe. Corrected reflectance spectra of 2 pixels correctly identified as blood, 2 false positives and 2 false negatives are depicted in Figure 3.11.

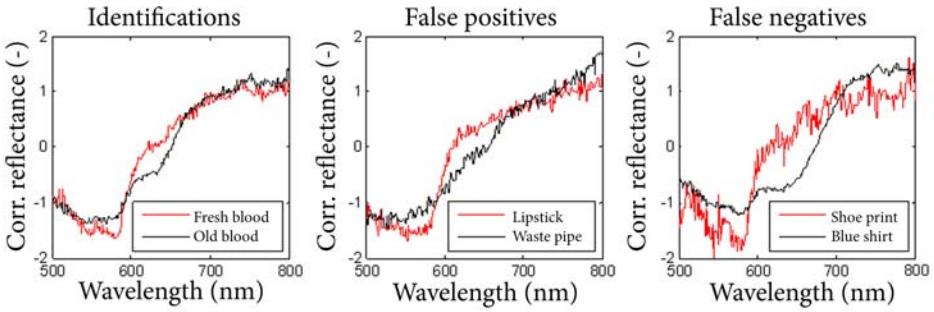


Figure 3.11. Corrected reflectance spectra of 2 pixels correctly identified as blood, 2 false positives and 2 false negatives.

## 3.4. DISCUSSION AND CONCLUSION

We demonstrated the feasibility to use spectroscopy or hyperspectral imaging to identify blood stains remotely. Based on their optical properties, both fresh and old blood stains from various donors were successfully distinguished from other samples, with a high specificity and sensitivity. No significant differences were found between blood stains for various samples or various donors. A small significant difference was found among blood stains with varying age. Yet, these differences did not hamper discrimination between blood and non-blood samples. In a case example, the absence of blood was determined using the described technique, which was confirmed by a tetrabase test. The practical applicability of this technique was demonstrated at a mock crime scene, where blood stains were identified automatically using hyperspectral imaging.

As illustrated by the ROC curve in Figure 3.9c there is a trade-off between sensitivity and specificity of this technique, which both depend on the choice of the threshold. In the spectroscopy setup for example, if no false positives are allowed, a possible threshold would be at $R^2$=0.97, resulting in a 100% sensitivity and a specificity of 98.1%. In forensic casework however, it seems more relevant to accept some false positives by choosing a threshold which leads to a 100% sensitivity, to prevent that blood stains are overlooked. When hyperspectral imaging was used, the specificity was 85% with a sensitivity of 100%. Because spectroscopy and hyperspectral imaging are non-

contact and non-destructive, all trace material is conserved and can be swabbed for subsequent confirmative identification tests in the laboratory.

The results of the identification task were somewhat better for probe based spectroscopy, compared to hyperspectral imaging, which can be explained by the larger sampled area. Averaging hyperspectral imaging data from multiple pixels covering the same area is expected to lead to better results. The $R^2$ values between measured reflectance spectra and non-linear least squares fits of the haemoglobin components were in general higher for the hyperspectral imaging measurements, which was expected as a result of the added Standard Normal Variate correction applied in this case. When using hyperspectral imaging, we observed higher $R^2$ values in the laboratory data than in the mock crime scene data, which may be explained by geometrical parameters like object to sensor distance and angle.

Regardless the results, hyperspectral imaging has benefits compared to probe based spectroscopy. Because both spectral and spatial information are recorded, traces can be analysed within their original context. Additionally, it is less labour-intensive and more time-efficient; an entire crime scene can be captured rapidly using a hyperspectral imaging system. The hyperspectral image of the mock crime scene presented in this study was recorded within two minutes. Although the subsequent pixel-based calculation time was several hours, this can easily be reduced using preliminary data reduction steps.

In casework traces are typically not found on ideal full-reflecting backgrounds used in laboratories, but all possible backgrounds can be encountered (e.g. different materials, porous, non-porous, coloured, patterned, etc.). Results of the mock crime scene showed that some backgrounds complicate the analysis. Several blood stains on the cloth on the floor, which appeared to be thinner, were not identified. This failure may be explained by the higher contribution of the background to the measured reflectance spectra in these pixels. Additionally, the absorption by the background complicated the measurements on the blue T-shirt. For dark backgrounds which absorb most visible light, near infrared spectroscopy can be used for the identification of blood stains, as shown in **Chapter 7**[19]. In **Chapter 5**, the influence of different

backgrounds and the limitations of the visible wavelength range will be explored.

Other errors in the hyperspectral imaging setup were caused by specular reflections. Sunlight, external light sources, shadows and reflections from nearby objects all change the apparent illumination on an object. This variation can cause large variability in the measured spectra for a fixed object, a problem regularly encountered in remote sensing. In this study, we applied a correction algorithm for differences in offset and intensity of the reflectance spectra, which greatly reduced the variability between samples measured at various distances from the sensor, where the local intensity of the light source varied[67]. However, more algorithms may be needed to correct for other effects encountered in complex crime scenes.

We show the possibility to estimate the age of blood stains using hyperspectral imaging in **Chapter 4**[49]. Combined with the technique described above, it is possible to simultaneously detect and identify blood stains and estimate their age non-destructively. When introduced in forensic casework, the described technique can help investigators to analyse traces in the original context at the crime scene, without the need to wait for results from the laboratory. This helps investigators to select most relevant traces, which reduces the workload in forensic laboratories.

## 3.5. ACKNOWLEDGEMENTS

Part of this research was developed in the project CSI the Hague, within the Pieken in de Delta program by the NL Agency of the Dutch Ministry of Economic Affairs, Agriculture and Innovation (project number PID082036).